Ab initio study of the structural, electronic and elastic properties of AgSbTe2, AgSbSe2, Pr3AlC, Ce3AlC, Ce3AlN, La3AlC and La3AlN compounds

ARTICLE *in* PHYSICA B CONDENSED MATTER · SEPTEMBER 2012

Impact Factor: 1.32 · DOI: 10.1016/j.physb.2012.04.011

3 AUTHORS:

Saadi Berri
University of Setif, 19000 Setif, Algeria
16 PUBLICATIONS **46** CITATIONS
SEE PROFILE

D. Maouche
Ferhat Abbas University of Setif
47 PUBLICATIONS **263** CITATIONS
SEE PROFILE

Youcef Medkour
University of Setif 1,Setif, Algeria
26 PUBLICATIONS **74** CITATIONS
SEE PROFILE

Physica B 407 (2012) 3320–3327

Contents lists available at SciVerse ScienceDirect

Physica B

journal homepage: www.elsevier.com/locate/physb

Ab initio study of the structural, electronic and elastic properties of $AgSbTe_2$, $AgSbSe_2$, Pr_3AlC, Ce_3AlC, Ce_3AlN, La_3AlC and La_3AlN compounds

S. Berri [a,*], D. Maouche [b], Y. Medkour [a]

[a] Department of Physics, Faculty of sciences, University of Setif, Algeria
[b] Laboratory for Developing New Materials and their Characterizations, University of Setif, Algeria

ARTICLE INFO

Article history:
Received 22 November 2011
Received in revised form
23 March 2012
Accepted 5 April 2012
Available online 25 April 2012

Keywords:
Chalcogenides
Antiperovskite
Ab initio calculations
Electronic structure
Elastic constants

ABSTRACT

In this paper, we study the structural, electronic and elastic properties of the ternary $AgSbTe_2$, $AgSbSe_2$, Pr_3AlC, Ce_3AlC, Ce_3AlN, La_3AlC and La_3AlN compounds using the full-potential linearized augmented plane wave (FP-LAPW) scheme and the pseudopotential plane wave (PP-PW) scheme in the frame of generalized gradient approximation (GGA). Results are given for the lattice parameters, bulk modulus, and its pressure derivative. The calculated lattice parameters are in good agreement with experimental results. We have determined the full set of first-order elastic constants, shear modulus, Young's modulus and Poisson's ratio of these compounds. Also, we have presented the results of the band structure, densities of states, it is found that this compounds metallic behavior, and a negative gap $\Gamma \rightarrow R$ for Pr_3AlC. The analysis charge densities show that bonding is of covalent–ionic and ionic nature for $AgSbSe_2$ and $AgSbTe_2$ compounds.

1. Introduction

The ternary chalcogenides $AgSbSe_2$ and $AgSbTe_2$ belong to the family of semiconductors with a disordered NaCl cubic structure; $AgSbTe_2$ is not only a good thermoelectric but is the end compound of several high-temperature, high-performance thermoelectric [1–4]. The electrical conductivity measurements [5] show a metallic behavior of $AgSbTe_2$, whereas the diffuse reflectance suggests an apparent band gap (0.35 eV). A similar observation in the diffuse reflectance spectrum of $AgSbSe_2$ has also been made (see Ref. [6]). $AgSbX_2$ (X=Se,Te) compounds are related to zinc-blende structures. Rock salt $AgSbSe_2$ and $AgSbTe_2$ were synthesized in 1957 [7]. The Ag compounds show an importance in thermoelectric, optical phase change, and frequency conversion applications [8,9]. In comparison with the classical GeSbTe phase change memory alloy, AgVInSbTe is reported to have better erasability and cyclability in memory switching [10–13]. Experimentally Kumar et al. [14,15] found that the compounds under study have undergone a transition phase from B1 to B2 between 17 and 26 GPa for $AgSbTe_2$ and 15 GPa for $AgSbSe_2$. A transition under temperature was observed from solids to liquids at $T=849$ K for $AgSbTe_2$ and $T=909.5$ K for $AgSbSe_2$ [16]. In recent years the perovskite ABX_3 type compounds have numerous technological applications due to their wide range of attractive properties, ferroelectricity [17–19], piezoelectricity [20,21], semiconductivity [22], catalytic activity [23], and thermoelectricity [24], superconductivity and metal–insulator transition [25]. Example ternary oxides of rare earth (Eu,Gd and Tb)CoO_3 are important materials because of their electrical, magnetic and catalytic properties. The perovskite type oxides in this series find extensive application in materials science and technology, some of the perovskite (Eu,Gd and Tb)CoO_3

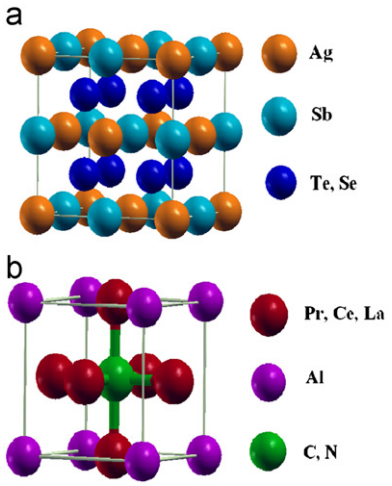

Fig. 1. Crystal structure of (a) $AgSbTe_2$ and $AgSbSe_2$, (b) Pr_3AlC, Ce_3AlC, Ce_3AlN, La_3AlC and La_3AlN compounds.

* Corresponding author. Tel.: +213 795115576; fax: +213 36 92 72 10.
E-mail address: berrisaadi12@yahoo.fr (S. Berri).

0921-4526/$ - see front matter © 2012 Elsevier B.V. All rights reserved.
http://dx.doi.org/10.1016/j.physb.2012.04.011

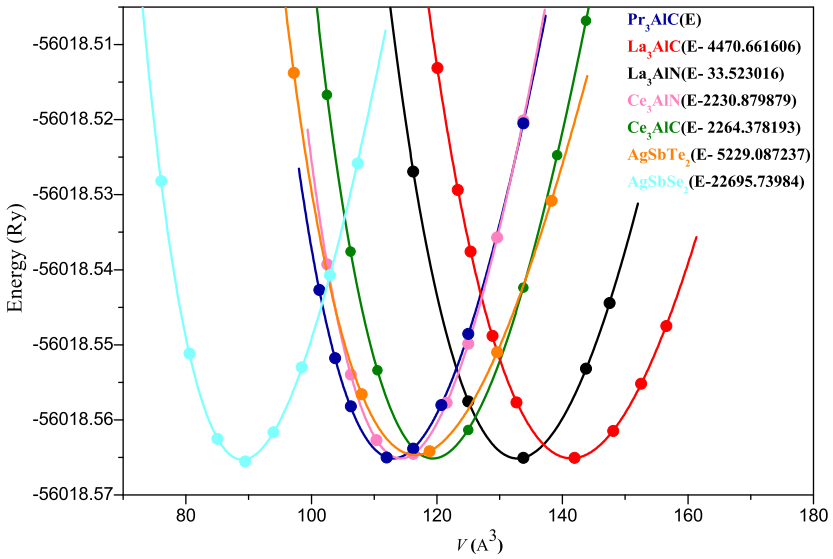

Fig. 2. Calculated total energies as a function of volume of $AgSbTe_2$, $AgSbSe_2$, Pr_3AlC, Ce_3AlC, Ce_3AlN, La_3AlC and La_3AlN compounds.

Table 1
Lattice constant a(Å), bulk modulus B (in GPa) pressure derivative of bulk modulus B' for $AgSbSe_2$, $AgSbTe_2$ Pr_3AlC, Ce_3AlC, Ce_3AlN, La_3AlC and La_3AlN compounds.

	Present work (FP-LAPW)	Present work (PW-PP)	Experiment	Others
$AgSbTe_2$				
a	6.4	7.4	6.2 [15] 6.078 [16]	5.93 [15] 5.676 [39] 6.29 [40]
B	51.34	56.87	45 [15]	44.5 [15]
B'	4.697	4.23	–	4.8 [15]
$AgSbSe_2$				
a	5.89	7.01	5.786 [16]	–
B	73.85	69.73	–	–
B'	4.33	4.12	–	–
La_3AlC				
a	5.21	4.979	5.109 [42]	–
B	55.241	72.715	–	–
B'	3.292	3.551	–	–
Ir_3WC [44]				
B	256	–	–	–
La_3AlN				
a	5.103	4.859	5.07 [41]	–
B	65.336	78.378	–	–
B'	3.559	4.102	–	–
Cu_3CdN[43]				
B	99.4	–	–	–
Ce_3AlN				
a	4.853	4.866	5.008 [41]	–
B	76.915	66.827	–	–
B'	4.201	3.927	–	–
Ce_3AlC				
a	4.924	4.917	5.007 [42]	–
B	68.608	71.648	–	–
B'	3.917	3.982	v	–
Pr_3AlC				
a	4.835	4.972	5.04 [42]	–
B	66.642	67.548	–	–
B'	3.805	3.975	–	–

Table 2
Calculated values of elastic constants Cij (in GPa).

	C_{11}	C_{12}	C_{44}
$AgSbTe_2$			
Present work (FP-LAPW)	55.32	43.38	2.51
Present work (PW-PP)	81.04 ± 4.12	44.5 ± 2.25	1.46 ± 0.09
$AgSbSe_2$			
Present work (FP-LAPW)	84.48	68.535	1.67
Present work (PW-PP)	100.9 ± 3.98	43.74 ± 1.55	2.95 ± 0.07
La_3AlC			
Present work (FP-LAPW)	97.15	35.88	29.14
Present work (PW-PP)	118.883 ± 4.82	40.568 ± 2.90	38.090 ± 0.10
La_3AlN			
Present work (FP-LAPW)	180	98	47
Present work (PW-PP)	209.441 ± 5.28	31.065 ± 2.87	48.397 ± 0.08
Ce_3AlN			
Present work (FP-LAPW)	259	120	33
Present work (PW-PP)	261.037 ± 4.18	64.127 ± 2.71	0.08 ± 42.335
$RuFe_3N$ [45]			
(PW-PP)	363	87.4	117
Ce_3AlC			
Present work (FP-LAPW)	269	125	88
Present work (PW-PP)	312.27 ± 3.98	197 ± 2.41	71.32 ± 0.05
Ir_3WC [44]			
(FP-LAPW)	355	207	17
Pr_3AlC			
Present work (FP-LAPW)	381	208	101
Present work (PW-PP)	412.117 ± 4.07	217.2 ± 2.99	97.12 ± 12

compounds are used as electrode materials for magnetohydrodynamic (MHD) generators [26] and for fuel cells [27]. In general, $AgSbSe_2$ and $AgSbTe_2$ compounds crystallize in the cubic space group Fm3m(#225) [16]. The Ag atom are positioned at the (0 0 0) position, the Sb atom at the (0.5 0.5 0.5) position and Se or Te atom at the (0.25 0.25 0.25) position. On the other hand the compounds ABX_3 crystallize in the cubic space group Pm3m(#221) [28]. The Al atom is positioned at the (0 0 0) position, the C or N atom at the (0.5 0.5 0.5) position, and Pr, Ce or La atom occupies the position (0 0.5 0.5). The crystal structure of these compounds is shown in Fig. 1. Today, there are no theoretical reports on the physical properties of Pr_3AlC, Ce_3AlC, Ce_3AlN, La_3AlC and La_3AlN compounds in the literature. Our paper is organized as follows. The theoretical background is presented in Section 2 and the results are presented in Section 3. Finally, a summary is given in Section 4.

2. Method of calculations

To obtain these results we have employed first principles calculations [29,30] with both the full potential linear augmented plane wave (FP-LAPW) method [31] as implemented in the WIEN2k code [32] and the pseudopotential plane wave (PP-PW) scheme in the frame of generalized gradient approximation (GGA). The exchange–correlation effects were described with the parameterization of Perdew et al. (GGA-PBE) [33]. In the calculations reported here, we use a parameter $R_{mt}K_{max}=9.5$, which determines the matrix size (convergence), where K_{max} is the plane wave cut-off and R_{mt} is the smallest of all atomic sphere radii. We have chosen the muffin-tin radii (MT) for Ag, Sb, Te, Se, Pr, Ce, La, Al, N and C to be 2.2, 2.3, 2.4, 2.1, 2.45, 2.35, 2.3, 2.25, 1.9 and 1.8 (a.u) respectively. Within these spheres, the charge density and potential are expanded in terms of crystal harmonics up to angular momenta $L=10$, and a plane wave expansion has been used in the interstitial region. The value of $G_{max}=14$, where G_{max} is defined as the magnitude of largest vector in charge density Fourier expansion. The Monkorst–Pack special k-points were performed using 35 special k-points in an irreducible Brillouin zone (IBZ) [34]. The convergence criteria for total energy and force are taken as 10^{-5} and 10^{-4} eV/Å, respectively.

We have used the norm-conserving pseudopotential (NCP) method [35] and the generalized gradient approximation according to (PBE) [33] were performed using the computer program CASTEP (Cambridge Serial Total Energy Package) [36]. To calculate structural, elastic, and electronic properties for $AgSbTe_2$, $AgSbSe_2$, Pr_3AlC, Ce_3AlC, Ce_3AlN, La_3AlC and La_3AlN compounds. The kinetic cut-off energy for the plane wave expansion is taken to be 600 eV. The special points sampling integration over the Brillouin zone was employed by using the Monkhorst–Pack method with a $7\times7\times7$ special k-point mesh [34]. Based on the Broyden Fletcher Goldfarb Shenno (BFGS) [37] minimization technique, the system reached the ground state via self-consistent calculation when the total energy is stable to within 5×10^{-6} eV/atom, and less than 10^{-2} eV/Å for the force. These parameters were sufficient in leading to well converged total energy, geometrical configurations and elastic moduli.

Table 3
Shear modulus G, Young's modulus E (GPa), Poisson's ration v and Lamé's.

	G	E	v	μ	λ
$AgSbTe_2$					
Present work (FP-LAPW)	3.89	11.4	0.46	3.89	0.27
Present work (PW-PP)	1.46	49.49	0.35	1.46	78.12
$AgSbSe_2$					
Present work (FP-LAPW)	4.19	12.34	0.47	4.19	0.22
Present work (PW-PP)	2.94	74.44	0.3	2.94	95.01
La_3AlC					
Present work (FP-LAPW)	29.738	75.64	0.271	29.738	7.378
Present work (PW-PP)	38.09	98.239	0.254	38.09	42.702
La_3AlN					
Present work (FP-LAPW)	44.6	108.998	0.221	44.6	11.009
Present work (PW-PP)	48.397	201.416	0.129	48.397	112.647
Ce_3AlN					
Present work (FP-LAPW)	47.6	118.379	0.243	47.6	11.891
Present work (PW-PP)	64.78	146.87	0.133	64.78	12.62
$RuFe_3N$ [45]					
(PW-PP)	100.3	258	0.284	–	–
Ce_3AlC					
Present work (FP-LAPW)	81.6	175.301	0.074	81.6	10.306
Present work (PW-PP)	65.6	150.78	0.142	65.6	13.73
Pr_3AlC					
Present work (FP-LAPW)	95.2	193.472	0.16	95.2	2.971
Present work (PW-PP)	99.6	200.33	0.12	99.6	18.37

Coefficients μ and λ (GPa) for $AgSbSe_2$, $AgSbTe_2$, La_3AlC, La_3AlN, Ce_3AlN, Ce_3AlC, and Pr_3AlC compounds.

3. Results and discussion

3.1. Structural properties

We have calculated the total energy of $AgSbTe_2$ and $AgSbSe_2$, Pr_3AlC, Ce_3AlC, Ce_3AlN, La_3AlC and La_3AlN using FP-LAPW and PP-PW methods. The plots of calculated total energies versus reduced volume for these compounds are given in Fig. 2. The total energies versus changed volumes are fitted to Murnaghan's equation of state [38] in order to determine the ground state properties, such as equilibrium lattice constant a, bulk modulus B and its pressure derivative B'. The calculated structural parameters for these compounds are summarized in Table 1, together with the available experimental and theoretical results for comparison. Our results for lattice parameters and bulk modulus for $AgSbTe_2$ and $AgSbSe_2$ are in good agreement with previous theorical [9,15,39] and available experimental data [15,16]. The obtained results

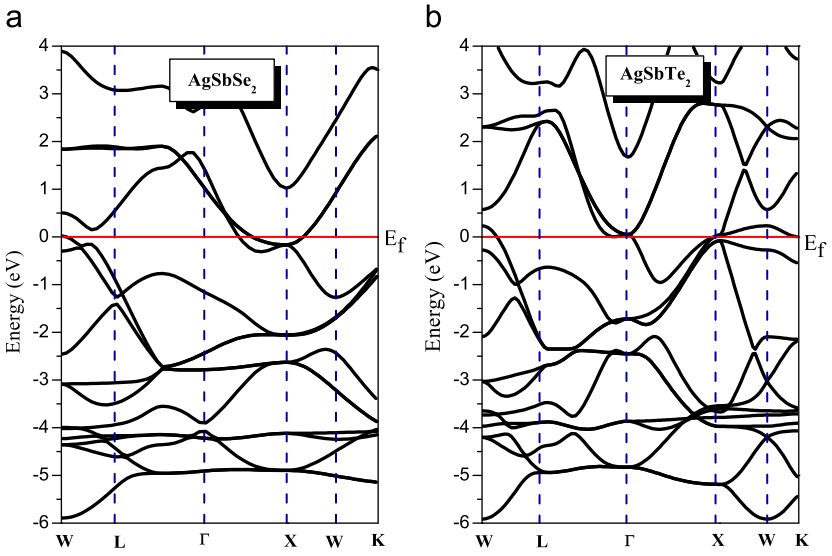

Fig. 3. Band structure for high-symmetry directions in the Brillouin zone of $AgSbSe_2$ and $AgSbTe_2$ compounds.

with the FP-LAPW method are in better agreement with the experimental data compared to those calculated by the PP-PW method. On the other hand, the results for lattice parameters of Pr_3AlC, Ce_3AlC, Ce_3AlN, La_3AlC and La_3AlN compounds are in agreement with the experimental data [40,41] for both methods. In our knowledge there are no experimental works or theoretical calculations exploring the bulk modulus and its pressure derivative of these compounds, We also include in Table 1, the bulk modulus and its pressure derivative data for Cu_3CdN [42], and Ir_3WC [43] for comparison purpose.

3.2. Elastic properties

The elastic constants of solids are among the most fundamental properties, and give important information, such as interatomic bonding characteristic between adjacent atomic planes, equations of

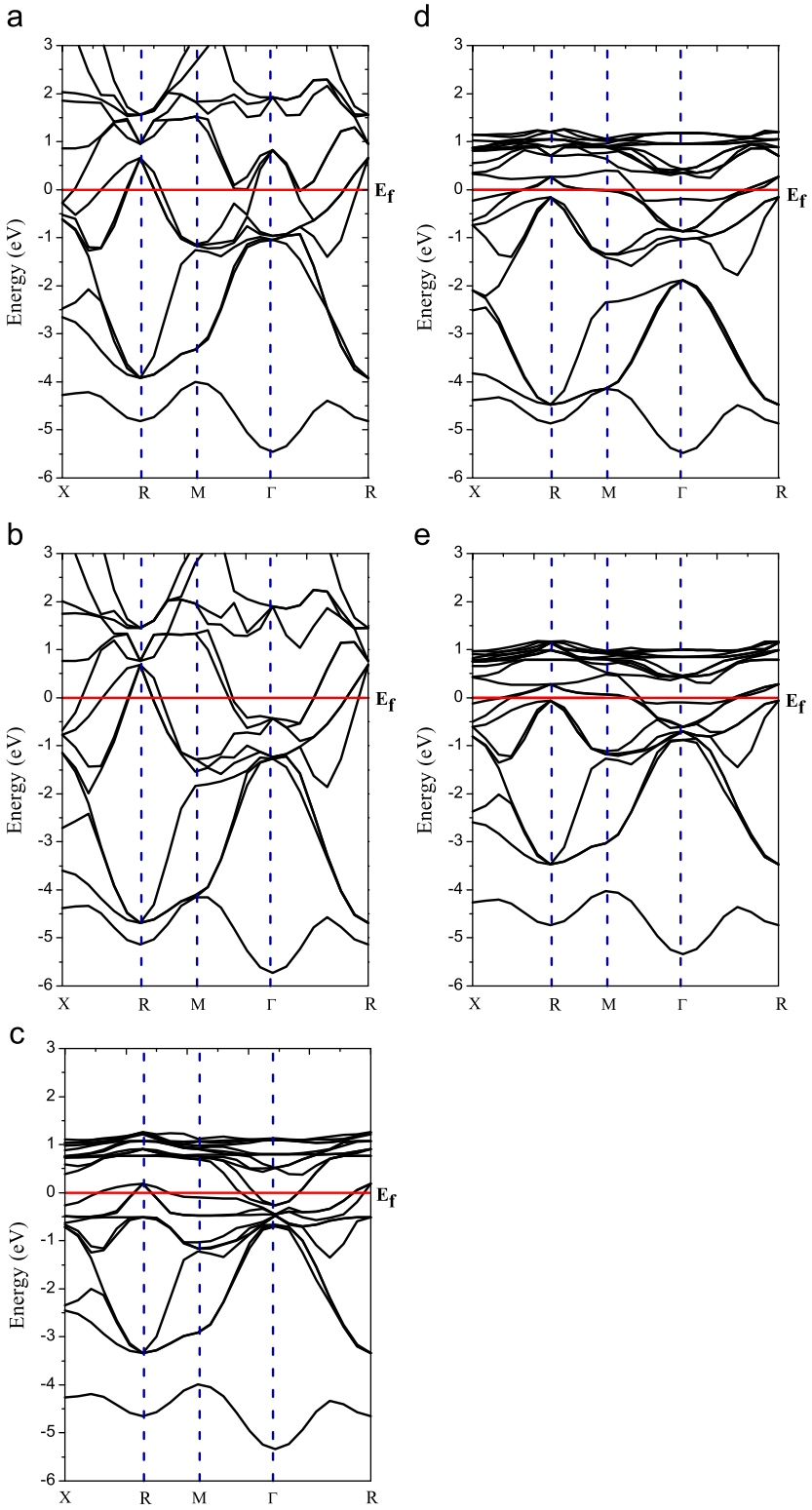

Fig. 4. Band structure for high-symmetry directions in the Brillouin zone of (a) La_3AlC, (b) La_3AlN, (c) Pr_3AlC, (d) Ce_3AlN and (e) Ce_3AlC compounds.

state, and phonon spectra [44]. That can be predicted from first-principles ground-state total-energy calculations. The elastic constants C_{ij} are the proportionality coefficients relating the applied strain to the computed stress, $\sigma_i = C_{ij}\varepsilon_i$. So, to study the stability of these compounds, we have calculated the elastic constants with both methods. It is well known that a cubic crystal has only three independent elastic constants, C_{11}, C_{12} and C_{44}. Hence, a set of three equations is needed to determine all constants. The first equation involves calculating the elastic constants C_{11} and C_{12} which are related to the bulk modulus B.

$$B = \frac{1}{3}(C_{11}+2C_{12}) \tag{1}$$

The second one involves applying volume-conserving tetragonal strains

$$\bar{\varepsilon} = \begin{pmatrix} \varepsilon & 0 & 0 \\ 0 & \varepsilon & 0 \\ 0 & 0 & \frac{1}{1+\varepsilon}-1 \end{pmatrix} \tag{2}$$

Application of this strain changes the total energy from its initial value as follows:

$$E(\gamma) = (C_{11}-C_{12})6V_0\gamma^2 + 0(\gamma^3) \tag{3}$$

where V_0 is the volume of the unit cell. Finally, for the last type of deformation, we used the volume-conserving rhombohedral strain tensor given by

$$\bar{\varepsilon} = \begin{pmatrix} 1 & \frac{\varepsilon}{2} & 0 \\ \frac{\varepsilon}{2} & 1 & 0 \\ 0 & 0 & \frac{4}{(4-\varepsilon^2)} \end{pmatrix} \tag{4}$$

which transform the total energy to the full elastic tensor.

$$E(\gamma) = \frac{V_0}{3}(C_{11}+2C_{12}+4C_{44}) + 0(\gamma^3) \tag{5}$$

We also calculate the shear modulus G, Young's modulus E, Poisson's ration v and Lamé's coefficients (μ and λ), which are frequently measured for polycrystalline materials when investigating their hardness. These quantities are related to the elastic constants by the following equations:

$$E = 9\beta G/(3\beta+G) \tag{6}$$

$$G = (C_{11}-C_{12}+3C_{44})/5 \tag{7}$$

$$v = (3\beta-E)/(6\beta) \tag{8}$$

$$\mu = E/(2(1+v)) \tag{9}$$

$$\lambda = vE/((1+v)(1-2v)) \tag{10}$$

The calculated elastic constants (C_{11}, C_{12} and C_{44}) are given in Table 2, the shear modulus G, Young's modulus E, Poisson's ratio v and Lamé's coefficients (μ and λ) are given in Table 3.

The value of the Poisson's ratio is small ($v=0.1$) for covalent materials, whereas for ionic materials 0.25, i.e, is a typical value of v [45]. For Ce_3AlN and La_3AlN compounds, the values of the Poisson ratio v of about ≈ 0.22 for FP-LAPW and ≈ 0.12 for PP-PW methods. In the case of Pr_3AlC compound the values of the Poisson ratio v is equal to ≈ 0.12, which indicates that higher covalent contribution in inter-atomic bonding.

On the other hand,the $AgSbTe_2$ and $AgSbSe_2$ compounds, have the largest Poisson's ratio of about ≈ 0.4 for FP-LAPW and ≈ 0.3 for PP-PW methods, and $v \approx 0.25$ of La_3AlC for both methods, indicates that $AgSbTe_2$, $AgSbSe_2$, Pr_3AlC, Ce_3AlN, La_3AlC and La_3AlN compounds as an ionic materials. We can observe that for Ce_3AlC, the values of the Poisson ratio v of about 0.074 for FP-LAPW and 0.142 for PP-PW methods.

Young's modulus is defined as the ratio of stress and strain, and is used to provide a measure of stiffness of the solid. When the value of E is large, the material is stiff [44].

Young's modulus of $AgSbSe_2$ is higher than that of $AgSbTe_2$, for two methods. For, Pr_3AlC, Ce_3AlC, Ce_3AlN, La_3AlC and La_3AlN compounds, the value's of Young's modulus are found to be 201.416 GPa for La_3AlN and 193.472 GPa for Pr_3AlC by using PW-PP and FP-LAPW methods respectively.

From Table 2, we can observe that the shear modulus G decreases in the following sequence: $La_3AlC \rightarrow La_3AlN \rightarrow Ce_3AlN \rightarrow Ce_3AlC \rightarrow Pr_3AlC$ and $AgSbTe_2 \rightarrow AgSbSe_2$ in both methods. Since there are no results available for the elastic constants, the shear modulus G, Young's modulus E, Poisson's ratio v and Lamé's coefficients (μ and λ), a comparison was performed with the $RuFe_3N$ [46]. The difference in value the elastic constants between the two methods is mainly due to the difference in methods.

The requirement of mechanical stability in this cubic structure leads to the following restrictions on the elastic constants:

$$C_{11}-C_{12} > 0,\ C_{44} > 0,\ C_{11}+2C_{12} > 0 \tag{11}$$

The ternary $AgSbTe_2$, $AgSbSe_2$, Pr_3AlC, Ce_3AlC, Ce_3AlN, La_3AlC and La_3AlN compounds investigated here are based on cubic structures. Our results satisfy all the criteria, and it follows that these criteria in Eq. (11) are satisfied, and it follows that these materials are stable.

3.3. Electronic structure

3.3.1. Band structure

The band structures for those compounds have been calculated at the theoretical equilibrium lattice constant by using FP-LAPW and PP-PW methods along high-symmetry directions of the first Brillouin zone are plotted in Figs. 3 and 4. Note that, there is no difference in the band structure plot for the two methods.

The conduction band minimum (CBM) is found to be mixed with the valence band maximum (VBM) along the (XX) direction for $AgSbTe_2$ and $AgSbSe_2$ from the two methods. The experimental value of the band gap for $AgSbTe_2$ is 0.71 eV, obtained by using

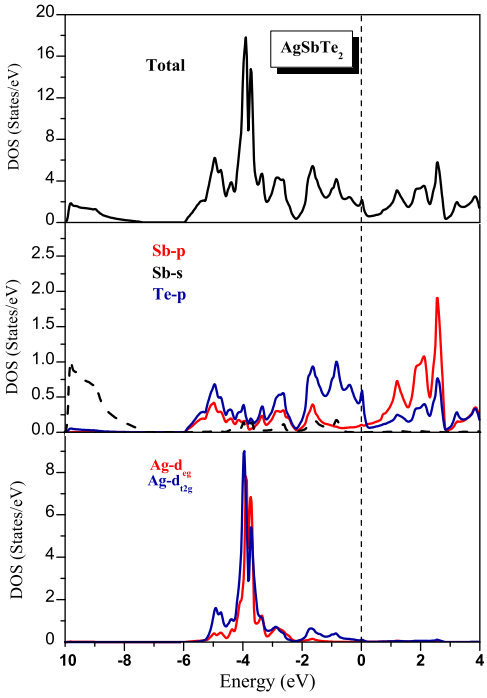

Fig. 5. Total and partial DOS of $AgSbTe_2$ compounds.

direct gap-optical measurements [47,48]. While Abdel-ghany et al. [49] found a band gap of 1.65 eV by using indirect gap-optical measurements. For $AgSbSe_2$, a band gap value of 0.091 eV and 0.34 eV was found using electrical measurements [39], but the agreement with the experiments is still not perfect. One reason of this discrepancy is that in our calculations, we have

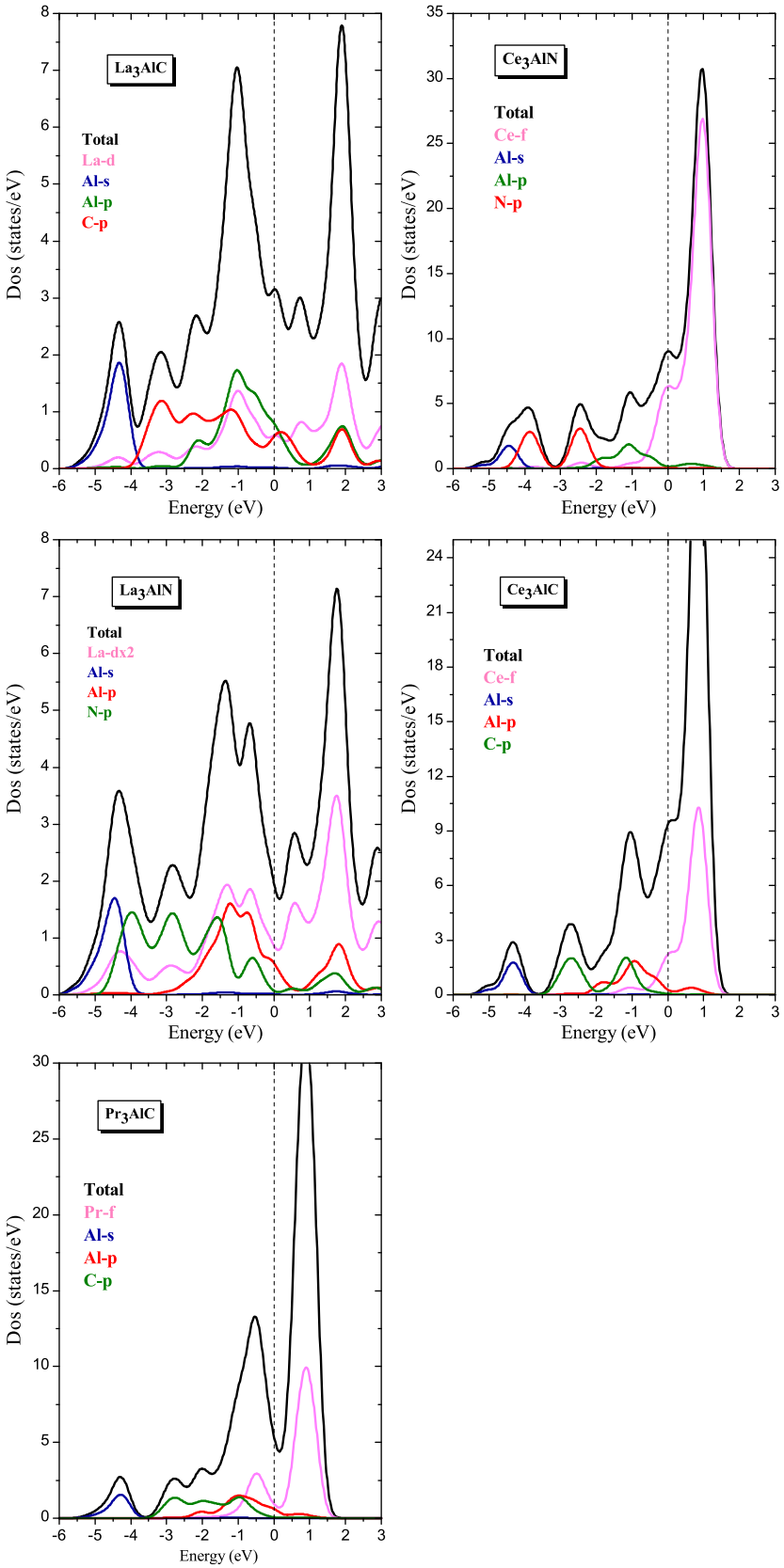

Fig. 6. Total and partial DOS of La_3AlC, La_3AlN, Pr_3AlC, Ce_3AlN and Ce_3AlC compounds.

assumed the crystal to be at $T=0$ K and thus do not include contributions from lattice vibrations that are present at room temperature measurements. On the other hand, from Fig. 4 we can see that La_3AlC, La_3AlN, Ce_3AlN and Ce_3AlC compounds have metallic behavior. In the case of Pr_3AlC phase the valence band maximum (VBM) is located at Γ point, whereas the conduction band minimum (CBM) is located at R point leads to a pseudogap of about −0.3 eV for FP-LAPW and −0.41 eV for PP-PW methods.

3.3.2. Total and partial density of states

To further elucidate the nature of the electronic band structure, we have calculated the total and the partial densities of states (DOS) of these compounds. These are displayed in Figs. 5 and 6. The density of states was presented only for $AgSbTe_2$ with the FP-LAPW method because it is similar to that of $AgSbSe_2$ and the PP-PW method with a small difference. It can be noted that the DOS of $AgSbTe_2$ can be mainly divided into three parts: the first part extending from −10 eV to −8 eV the contribution of Sb-s, the second part from −8 eV to 0 eV is of the combination of Ag (de_g and dt_{2g}) and Te-p and the third part extended from 0 eV to 4 eV, this structure originates from Sb-p states (see Fig. 5).

In the case La_3AlC, La_3AlN, Pr_3AlC, Ce_3AlN and Ce_3AlC compounds. The density of states was presented only with the FP-LAPW method because it is similar to that of the PP-PW method with a small difference, in Fig. 6. It can be noted that the DOS of La_3AlC, La_3AlN, Pr_3AlC, Ce_3AlN and Ce_3AlC compounds can be mainly divided into three parts: the first part extending from −6 eV to −4 eV is of the contribution of and Al-s states, the second part from −4 eV to 0 eV is the combination of p states of C or N Atom hybridized with Al-p orbital and the third part extended from 0 eV to 3 eV, this structure originates from La-d or f states of Ce or Pr atoms.

3.3.3. Charge density

In order to understand the nature of chemical bonding, we display, in Figs. 7 and 8, the contours of charge densities in the (1 1 0) plane for those compounds by using the FP-LAPW method. From Fig. 7, we can see that the near spherical charge distribution around the C and N atoms site are negligible and as a result the C and N atoms are fairly isolated, indicating that the bonding La–(C, N), Ce–(C, N) and Pr–C are expected to be some ionic character. On the other hand, the rare-earth (La, Ce and Pr) atoms hybridization with Al atom happens with a strong interaction between the rare-earth with Al atom. It is clear that a covalent interaction occurs between rare-earth (La, Ce and Pr) with Al atom. According to the correlation between the shear modulus, bulk modulus and

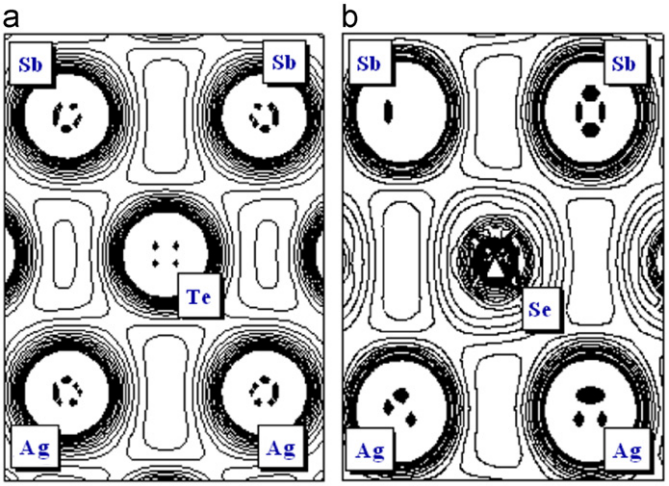

Fig. 8. Charge density distribution in the plan (1 1 0) of (a) $AgSbTe_2$, and (b) $AgSbSe_2$ compounds.

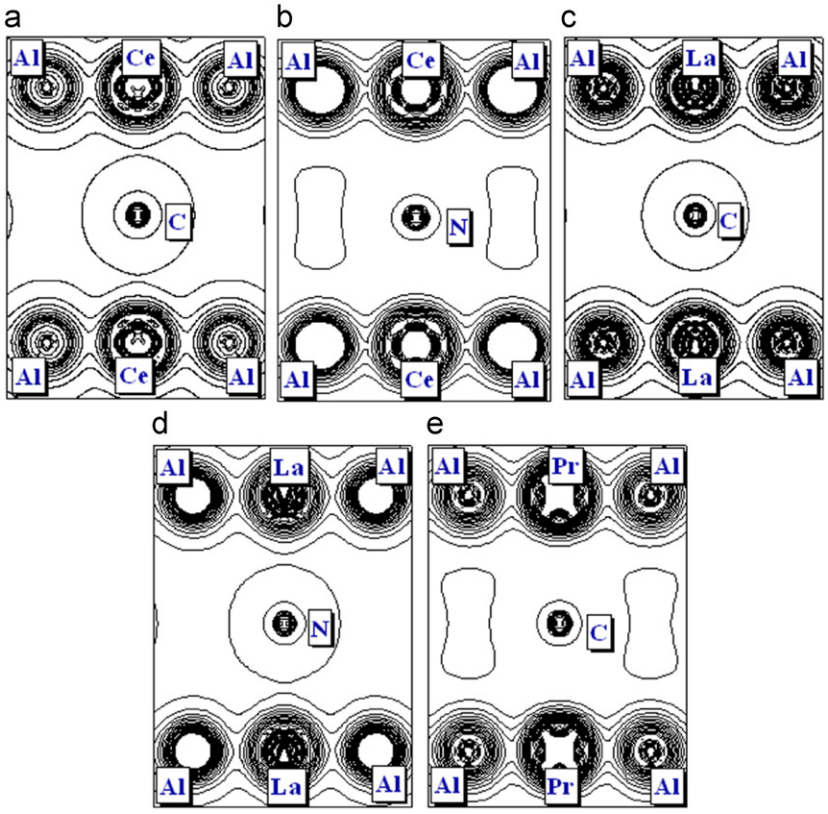

Fig. 7. Charge density distribution in the plan (1 1 0) of (a) Ce_3AlC, (b) Ce_3AlN, (c) La_3AlC, (d) La_3AlN and (e) Pr_3AlC compounds.

the hardness, it can be expected that Pr_3AlC will possess a high hardness compared to La_3AlC, La_3AlN, Ce_3AlN and Ce_3AlC compounds. The bonding character may be described as a mixture of covalent and ionic. In the case $AgSbSe_2$ and $AgSbTe_2$ compounds, the overall shape of the charge distributions suggests a partially ionic bonding in both Te–(Ag, Sb) and Se–(Ag, Sb) bonds (see Fig. 8). We can conclude that the bonding in $AgSbSe_2$ and $AgSbTe_2$ is a purely ionic character.

4. Conclusion

In the present work, we have used the FP-LAPW and PP-PW methods, implemented in the Wien2k and CASTEP within GGA, to obtain the structural, electronic and elastic properties of the ternary $AgSbTe_2$, $AgSbSe_2$, Pr_3AlC, Ce_3AlC, Ce_3AlN, La_3AlC and La_3AlN compounds. At $T=0$ K, the calculated lattice constants are in agreement with the experimental findings. The analysis of electronic structure showed that these compounds have a metallic character which allowed the Pr_3AlC compound to have an intermetallic behavior. We have calculated and analysis the elastic constants for these compounds, which have not been established previously theoretically and experimentally. The analysis of charge densities contours leads us to conclude that the bonding character in these compounds is a mixture between covalent–ionic and ionic nature for $AgSbSe_2$ and $AgSbTe_2$ compounds.

References

[1] C. Wood, Rep. Prog. Phys. 51 (1988) 459.
[2] K.F. Hsu, S. Loo, F. Guo, W. Chen, J.S. Dyck, C. Uher, T. Hogan, E.K. Polychroniadis, M.G. Kanatzidis, Science 303 (2004) 818.
[3] J. Androulakis, K.F. Hsu, R. Pcionek, H. Kong, C. Uher, J.J.D. Angelo, A. Downey, T. Hogan, M.G. Kanatzidis, Adv. Mater. 18 (2006) 1170.
[4] J. Androulakis, R. Pcionek, E. Quarez, J.H. Do, H. Kong, O. Palchik, C. Uher, J.J. D'Angelo, J. Short, T. Hogan, M.G. Kanatzidis, Chem. Mater. 18 (2006) 4719.
[5] R.M. Ayral-Marin, G. Brun, M. Maurin, J.C. Tedenac, Eur. J. Solid State Inorg. Chem. 27 (1990) 747.
[6] EPAPS Document No. E-PRLTAO-99-059741 for more details on the calculations, the structural properties, the energetics, the projected density of states analysis, sample preparation, and diffuse reflectance and magnetic susceptibility measurements that have not been given in the Letter. For more information on EPAPS, available from: 〈http://www.aip.org/pubservs/epaps.html〉.
[7] J.H. Wernick, K.E. Benson, Phys. Chem. Solids 3 (1957) 157.
[8] J. Feinleib, J. de Neufville, S.C. Moss, S.R. Ovshinsky, Appl. Phys. Lett. 18 (1971) 254.
[9] R. Detemple, D. Wamwangi, M. Wuttig, G. Bihlmayer, Appl. Phys. Lett. 83 (2003) 2572.
[10] J. Tominaga, T. Kikukawa, M. Takahashi, R.T. Phillips, J. Appl. Phys. 82 (1997) 3214.
[11] W.K. Njoroge, M. Wuttig, J. Appl. Phys. 90 (2001) 3816.
[12] J. Kalb, F. Spaepan, M. Wuttig, J. Appl. Phys. 93 (2003) 2389.
[13] N. Nobukini, M. Takashima, T. Ohno, M. Horie, J. Appl. Phys. 78 (1995) 6980.
[14] R.S. Kumar, A. Sekar, N.V. Jaya, S. Natarajan, J, Alloys Compd. 285 (1999) 48.
[15] R.S. Kumara, A.L. Corneliusa, E. Kima, Y. Shena, S. Yoneda, Ch. Chena, M.F. Nicol, Phys. Rev. B 72 (2005) 060101(R).
[16] S. Geller, J.H. Wernick, Acta Crystallogr (1959) 46.
[17] J.G. Bednorz, K.A. Muller, Phys. Rev. Lett. 52 (1984) 2289.
[18] C.B. Samantaray, H. Sim, H. Hwang, Microelectron. J. 36 (2005) 725.
[19] C.B. Samantaray, H. Sim, H. Hwang, Physica B 351 (2004) 158.
[20] P. Baettig, C.F. Schelle, R. Lesar, U.V. Waghmare, N.A. Spaldin, Chem. Mater. 17 (2005) 1376.
[21] H. Wang, B. Wang, Q. Li, Z. Zhu, R. Wang, C.H. Woo, Phys.Rev. B 75 (2007) 245209.
[22] H.P.R. Frederikse, W.R. Thurber, W.R. Hosler, Phys. Rev. 134 (1964) A442.
[23] C.S. Koonce, M.L. Cohen, J.F. Schooley, W.R. Hosler, E.R. Pfeiffer, Phys. Rev. 163 (1967) 380.
[24] V.E. Henrich, Rep. Prog. Phys. 48 (1985) 1481.
[25] L. Xiao-Juan, W. Zhi-Jian, H. Xian-Feng, X. Hong-Ping, J. Meng, Chem. Phys. Lett. 416 (2005) 7.
[26] D.B. Meadowcraft, P.G. Meier, A.C. Warren, Energy Convers. 12 (1972) 145.
[27] H.S. Spacil, C.S. Tedmon Jr., J. Electrochem. Soc. 116 (1969) 1618.
[28] F. Zhenbao, H. Haiquan, C. Shouxin, B. Chenglin, Solid State Commun. 148 (2008) 472.
[29] P. Hohenberg, W. Kohn, Phys. Rev. B 136 (1964) 864.
[30] W. Kohn, L.S. Sham, Phys. Rev. A 140 (1965) 113.
[31] J.C. Slater, Adv. Quantum Chem. 1 (1994) 5564.
[32] P. Blaha, K. Schwarz, G.K.H. Madsen, D. vasnicka, J. Luitz, WIEN2k: An Augmented Plane Wave Plus Local Orbitals Program for Calculating Crystal Properties, Vienna University of Technology, Vienna, Austria, 2001.
[33] J.P. Perdew, Y. Wang, Phys. Rev. B 45 (1992) 13244.
[34] H.J. Monkhorst, J.D. Pack, Phys. Rev. B 13 (1976) 5188.
[35] L. Klienman, D.M. Bylander, Phys. Rev. Lett. 48 (1982) 1425.
[36] M.D. Segall, P.J.D. Lindan, M.J. Probert, C.J. Pickard, P.J. Hasnip, S.J. Clark, M.C. Payne, J. Phys.: Condens. Matter 14 (2002) 2717.
[37] T.H. Fischer, J. Almlof, J. Phys. Chem. 96 (1992) 9768.
[38] F.D. Murnaghan, Proc. Natl. Acad. Sci. USA 30 (1944) 244.
[39] M. Luo, Adv. Mater. 16 (2004) 439.
[40] J.C. Schuster, J. Less-Common Met. 105 (1985) 327.
[41] T.M. Gesing, K.H. Wachtmann, W. Jeitschko, Z. Naturforsch. 52b (1997) 176.
[42] M.G. Moreno-Armenta, W.L. Pérez, N. Takeuchi, Solid State Sci. 9 (2007) 166.
[43] D.V. Suetin, I.R. Shein, A.L. Ivanovskii, Solid State Sci. 12 (2010) 814.
[44] E. Deligoz, H. Ozisik, K. Colakoglu, G. Surucu, Y.O. Ciftci, J. Alloys Compd. 509 (2011) 1711.
[45] V.V. Bannikov, I.R. Shein, A.L. Ivanovskii, Phys. Status Solidi 3 (2007) 89.
[46] E. Zhao, H. Xiang, J. Meng, Z. Wu, Chem. Phys. Lett. 449 (2007) 96.
[47] K. Wojciechowski, J. Tobola, M. Schmidt, R. Zybala, J. Phys. Chem. Solids 69 (2008) 2748. and references therein.
[48] H.A. Zayed, A.M. Ibrahim, L.I. Soliman, Vacuum 47 (1) (1996) 49.
[49] A. Abdel-ghany, S.N. El-sayed, D.M. Abdel-wahab, A.H. Abou El-Ela, N.H. Mousa, Electrical conductivity and thermoelectric power of $AgSbSe_2$, Mater. Chem. Phys. 44 (1996) 277.